Extreme-ultraviolet emission spectra of core-excited levels in sodium and magnesium

K. D. Pedrotti, A. J. Mendelsohn, R. W. Falcone,* J. F. Young, and S. E. Harris

Edward L. Ginzton Laboratory, Stanford University, Stanford, California 94305

Received May 13, 1985; accepted July 24, 1985

Using a pulsed-hollow-cathode discharge, we have observed the emission spectra of core-excited levels of Na I and Mg II. Line identifications and implications for extreme-ultraviolet lasers are discussed.

1. INTRODUCTION

As noted in an early paper by McGuire,[1] certain of the energy levels of Na I and Mg II that lie above a lower continuum and that have reasonably large radiative yields are of potential interest for the construction of extreme-ultraviolet (XUV) lasers. Depending on the speed of the excitation source relative to the Auger transition rate of the level, these levels may be excited either directly[2] or by store and transfer[3] from a metastable level.

During the past several years we have developed a pulsed-hollow-cathode discharge[4] that operates at a ground-level atom density of several Torr and that produces large densities of core-excited metastable atoms. Using this discharge, Holmgren has measured populations of 10^{11} atoms/cm^3 and 3×10^{10} atoms/cm^3 in the $2p^5 3s 3p\ {}^4D_{7/2}$ and $2p^5 3s 3p\ {}^4S_{3/2}$ levels of Na (Ref. 5) and in turn has used laser-induced fluorescence from these levels to develop a Grotrian diagram[6] for the three lowest configurations of the Na quartet system.

In this paper we give the results of a series of experiments in which a similar hollow-cathode discharge is used to take the XUV emission spectra of Na I and Mg II. The results complement the Holmgren research and also help to define XUV laser systems in these elements. Section 2 describes the experimental apparatus; Section 3 gives the emission spectra; line identifications are discussed in Section 4; and the implications for laser systems are discussed in Section 5.

2. EXPERIMENTAL APPARATUS

A schematic of the experimental apparatus is shown in Fig. 1. The radiation source consisted of a pulsed-hollow-cathode discharge similar to that described in Ref. 4. The discharge was run at a peak current of about 200 A, a peak voltage of 1 kV, and a pulse length of 4 μsec. The repetition rate was 100 Hz. For most operating conditions a dc simmer current of 5 mA was used to stabilize the discharge.

For the Na spectra the tube was run at 500°C with a He buffer of 1 Torr and a 304 stainless-steel cathode 1.3 cm in diameter and 5 cm long. Heat piping in Na is easily achieved, leading to a vapor zone whose pressure was equal to that of the He buffer gas that was used. The relatively high photoabsorption of He in the 400-nm region required that we run at the lowest possible buffer-gas pressure. This was found to be about 1 Torr.

For observation of the Mg II spectra an Ar buffer gas at a pressure of 2 Torr was used. Heat piping is difficult to achieve in Mg since its melting and boiling points are quite close, causing the Mg to solidify at the ends of the tube rather than to recirculate. The tube would thus periodically be depleted, necessitating reloading when run with a stainless-steel cathode. In order to avoid this problem and extend the running time of the source, some scans were made using a Mg cathode (3.8 cm long $\times$ 1 cm i.d.) with a dc simmer current of 0.5 A, which both heated the cathode evaporating the Mg and caused sputtering of the Mg. Ground-state densities between 10^{15} and 10^{16} were measured by using this method.

Radiation from the plasma entered the spectrometer through a 150-nm thick Al–Si filter mounted on electroformed Ni mesh (Luxel Corporation, Friday Harbor, Washington). This filter was used to isolate the high vacuum of the spectrometer from the heat-pipe oven. The filter has a transmission of ~50% between 18 and 40 nm. A McPherson Model 247 2.2-m grazing-incidence scanning monochromator evacuated to 10^{-7} Torr and equipped with a 300-line/mm grating blazed at 2.4° was used to gather the data. The detector was an EMI D233 windowless electron multiplier with the first Be–Cu dynode used as a photocathode. This detector has a quantum efficiently of 4% at 25 nm and 10% at 38.8 nm.[7] It was typically run at a voltage of 3500 V, yielding a gain of 5×10^6. The output of the detector was amplified and for the Mg scans was collected using a gated integrator (Stanford Research Systems Model SR250) and recorded on a strip-chart recorder. For the Na scans the detector output was amplified and the resulting photon pulses were counted using a discriminator and a dual-coincidence gate to allow counting only during times when the discharge was on and electrical noise was at a minimum. This resulted in a low spurious-count rate, which was due mostly to scattered light in the spectrometer and continuum emission. The inherent dark count rate of the detection system was 0.3 count per second. Periodically the counters were interrogated by a Z-80-based microcomputer system, which was used to collect, store, and display the spectra.

For some of the Na spectra a filter consisting of a thin film of 50 nm of Sb sandwiched between two 10-nm layers of Ti

0740-3224/85/121942-06$02.00

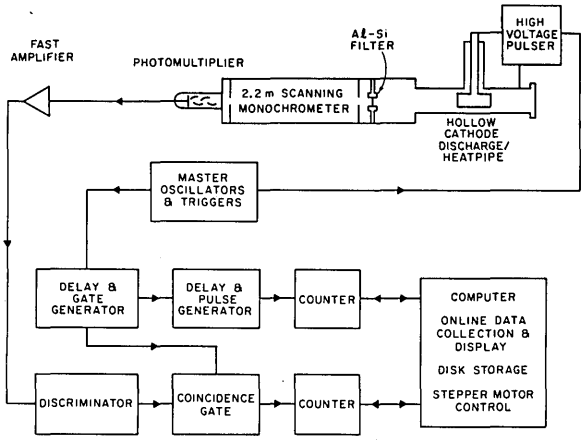

Fig. 1. Experimental apparatus.

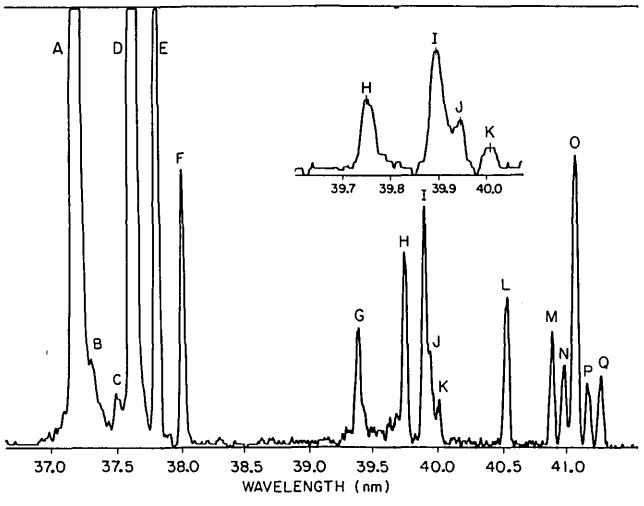

Fig. 2. Na emission spectrum.

mounted on electroformed Ni mesh was used to eliminate strong second-order Na ion lines (emitting at ~20 nm) from the region of interest around 40 nm. This filter transmitted from 35 to 55 nm with a peak transmission of 20% (detailed transmission curves are shown in Ref. 8). With the filter removed, the second-order replicas of ion lines were used to provide additional calibration throughout the region of interest. For the Mg scans an Al filter eliminated all possible second-order lines.

3. EXPERIMENTAL RESULTS

A. Sodium

The emission scans for Na are shown in Fig. 2. Table 1 lists the observed Na I features, and Table 2 lists the lines from higher stages of ionization. Calibration of the spectrometer was accomplished by fitting the cyclical error in the scan drive to known ion lines. Additional calibration lines were observed by removing the Ti–Sb–Ti filter. This procedure resulted in an error in the listed wavelengths of ±0.01 nm.

The wavelength predictions (λ pred.) shown in Table 1 were obtained from the calculations of Weiss[9] and the absorption measurements of Sugar *et al.*[010] as well as by combining the position of the $2p^53s3p\ ^4P_{5/2}$ level found in Ref. 10 with the accurate measurements of the relative quartet spacings made by Holmgren *et al.*[6]

The intensities listed are the number of counts observed in 4000 pulses at a slit width of 30 μm and are corrected for filter transmission. Correction is necessary since the filter transmission drops rapidly on the short-wavelength side of 40 nm.

For the Na I lines, the *A* coefficients and autoionizing times are computed using the RCN/RCG atomic-physics code.[12] The even-parity configurations included are $2p^53s3p$, $2p^53s4p$, $2p^53p4s$, and $2p^53p3d$. The odd-parity configurations included are $2p^53s3d$, $2p^53s4d$, $2p^53s5d$, $2p^53s^2$, $2p^53p^2$, and $2p^53s4s$.

B. Magnesium

The emission spectrum of Mg was recorded between 17 and 32 nm and is shown in Fig. 3. Table 3 lists our identifications of Mg II transitions. Lines that are due to higher ionization stages of Mg and of the buffer gas are shown in Table 4. The accuracy of these scans is ±0.02 nm, and the resolution is 0.1 nm.

A coefficients, autoionizing rates, and wavelengths were again computed using the RCN/RCG atomic-physics code. The even-parity configurations included were $2p^53s3p$, $2p^53s4p$, and $2p^53p4s$. The odd-parity configurations were $2p^53s^2$, $2p^53s4s$, $2p^53p^2$, $2p^53s3d$, and $2p^53s4d$.

Table 1. Na I XUV Decays

Line	λ Experiment (nm)	λ Predicted (nm)	Identification	Autoionizing Rate (sec^{-1})	Radiative Rate (sec^{-1})	Intensity (Corrected)
C	37.514	37.50[a]	$(2p^63d)^2P$–$[(2p^53s)^1P3d]^2D_{3/2}$ $(2p^63d)^2P$–$[(2p^53s)^1P3d]^2D_{5/2}$	3.4×10^{10} 2.2×10^{10}	3.5×10^9 3.7×10^9	895
G	39.394	39.384[b]	$(2p^63d)^2P$–$[2p^5(3s3p)^3P]^2P_{3/2}$	5.6×10^9	1.4×10^9	113
H	39.752	39.752[b]	$(2p^63p)^2P$–$[2p^5(3s3p)^3P]^4P_{5/2}$	3.8×10^{10}	2.3×10^8	282
I	39.898	39.898[c]	$(2p^63p)^2P$–$[2p^5(3s3p)^3P]^4D_{1/2}$	1.0×10^9	1.0×10^8	338
J	39.942	39.945[c]	$(2p^63p)^2P$–$[2p^5(3s3p)^3P]^4D_{3/2}$	1.8×10^{10}	1.4×10^8	152
K	40.014	40.003[c]	$(2p^63p)^2P$–$[2p^5(3s3p)^3P]^4D_{5/2}$	1.25×10^{10}	7.4×10^7	64
L	40.526	40.520[c]	$(2p^63p)^2P$–$[2p^5(3s3p)^3P]^4S_{3/2}$	4.2×10^5	9.6×10^6	190

[a] Ref. 9.
[b] Ref. 10.
[c] Refs. 6 and 10.

Table 2. Other Na Decays

Line	λ Experiment (nm)	λ Predicted[a] (nm)	Identification	Intensity (Corrected)
A	37.2074	37.2074	Na II $(2p^6)^1S_0$–$2p^5(^2P^\circ_{1/2})3s\,\frac{1}{2}\left[\frac{1}{2}\right]^\circ_{J=1}$	291 201
B	37.322	?	?	
D	37.6377	37.6377	Na II $(2p^6)^1S_0$–$2p^5(^2P^\circ_{3/2})3s\,\frac{3}{2}\left[\frac{3}{2}\right]^\circ_{J=1}$	492 168
E	37.814	37.8143	Na III $(2s^22p^5)^2P^\circ_{3/2}$–$(2s2p^6)^2S_{1/2}$	25 172
F	38.011	38.0107	Na III $(2s^22p^5)^2P^\circ_{1/2}$–$(2s2p^6)^2S_{1/2}$	12 502
M	40.868	40.8682	Na IV $(2s^22_p{}^4)^3P_2$–$(2s2p^5)^3P_1$	131
N	40.964	40.9615	Na IV $(2s^22p^4)^3P_1$–$(2s2p^5)^3P_0$	93
O	41.043	41.0371 41.0540	Na IV $(2s^22p^4)^3P_2$–$(2s2p^5)^3P_2$ Na IV $(2s^22p^4)^3P_1$–$(2s2p^5)^3P_1$	356
P	41.144	41.1333	Na IV $(2s^22p^4)^3P_0$–$(2s2p^5)^3P_1$	95
Q	41.237	41.2240	Na IV $(2s^22p^4)^3P_1$–$(2s2p^5)^3P_2$	120

[a] Ref. 11.

4. DISCUSSION

A. Sodium

Our identification of the Na I lines is based primarily on the research of Holmgren *et al.*[6] Holmgren used laser-induced fluorescence to measure accurately the relative positions of quartets in the $2p^53s3p$ and $2p^53s3d$ configurations. Combining these relative positions with the measurement of Sugar *et al.*[10] of the $2p^63p \rightarrow 2p^5(3s3p\ ^3P)^4P_{5/2}$ transition at 39.752 ± 0.002 nm allows the wavelength of the XUV quartet transitions to be predicted accurately.

In addition, rough intensity predictions were made based on *A* coefficients and autoionizing times calculated using the RCN/RCG atomic-physics code. These figures were used to compare the relative intensities of the Na I lines as well as to compare intensities with known Na II lines that are observed in both the XUV and visible regions.

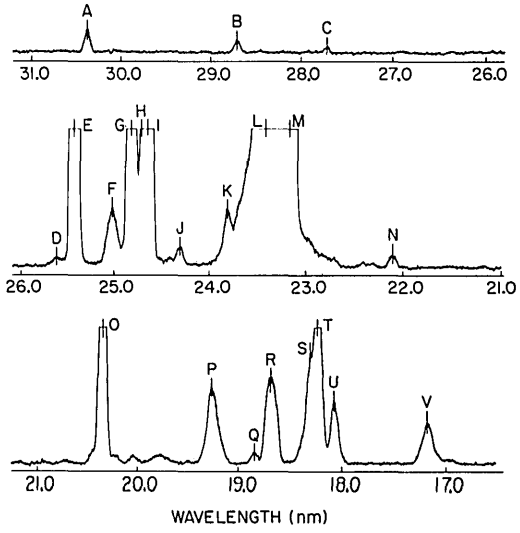

Fig. 3. Mg emission spectrum.

The quartet lines at 39.898 and 40.526 nm were previously observed, although not all identified, by Willison *et al.*[19] using a low-pressure microwave discharge. The decays at 40.526 nm and near 40 nm were observed in a lower-resolution emission spectrum by Zhmenyak *et al.*[20] Pegg *et al.*[13] have seen decay of the $(2p^53s3p)^4S$, ^4P, ^4D terms using ejected-electron spectroscopy.

The doublet transition at 37.514 nm is identified on the basis of its large intensity as predicted by the RCN/RCG code and the wavelength calculation of Weiss.[9] The doublet line at 39.394 nm was previously seen by Sugar *et al.*[10]

Of particular interest is the line at 40.526 nm, which we attribute to radiation from the $2p^53s3p\ ^4S_{3/2}$ level. Note that the intensity of this line is comparable with the other quartet decays even though its calculated *A* coefficient is over an order of magnitude less than those of other lines. This is because of its small autoionizing rate, which results from its first-order spin–orbit coupling only to nonautoionizing doublets.[21]

B. Magnesium

The present research represents the highest-resolution emission spectra of Mg II in this wavelength region to date. Our results for the decays of the doubly excited levels of Mg II will be discussed configuration by configuration.

The most interesting decays are those from the $2p^53s3p$ configuration. The lines at 25.44 and 24.66 nm are attributed to the decay of the $2p^53s3p\ ^4S_{3/2}$ and $2p^53s3p\ ^2P_{3/2}$ levels to the $2p^63p\ ^2P$ term. The identification of the lower level is confirmed by the observation of lines at 28.71 and 27.72 nm from these levels to the $2p^64p\ ^2P$ term. The $2p^53s3p\ ^4S_{3/2}$ level was seen previously as a small peak in the ejected-electron spectra of Pegg *et al.*[13] This is consistent with the slow autoionization rate calculated by both McGuire[1] and us for this level. The other significant decay from this configuration appears at 25.02 nm, which we attribute to the $2p^53s3p\ ^4D$ term decaying to the $2p^63p\ ^2P$ term, in agreement with Pegg *et al.*[13]

Table 3. Mg II XUV Decays

Line	λ Experiment (nm)	λ Other Experiment (nm)	Identification	Autoionization Rate (sec^{-1})[a]	Radiative Rate (sec^{-1})[a]	Intensity (arb. units)
B	28.71	–	$(2p^64p)^2P$–$(2p^53s3p)^4S_{3/2}$	9.5×10^4	1.4×10^4	2
C	27.72	–	$(2p^64p)^2P$–$[(2p^53s)^1P]3p^2P_{3/2}$	9.2×10^8	2.1×10^6	1
E	25.44	25.42[b]	$(2p^63p)^2P$–$(2p^53s3p)^4S_{3/2}$	9.5×10^4	2.1×10^7	140
F	25.02	25.04[b]	$(2p^63p)^2P_{3/2}$–$(2p^53s3p)^4D_{5/2}$ $(2p^63p)^2P$–$(2p^53s3p)^4D_{3/2}$ $(2p^63p)^2P$–$(2p^53s3p)^4D_{1/2}$	1.7×10^9 2.3×10^9 4.2×10^9	1.7×10^8 3.0×10^8 2.3×10^8	9
G	24.83	24.847[c]	$(2p^63s)^2S_{1/2}$–$(2p^53s^2)^2P^\circ_{3/2}$	9.5×10^{11}	4.0×10^9	68
H	–	24.714[c]	$(2p^63s)^2S_{1/2}$–$(2p^53s^2)^2P^\circ_{1/2}$	9.6×10^{11}	4.1×10^9	34
I	24.66	24.66[b]	$(2p^63p)^2P$–$[(2p^53s)^1P]3p^2P_{3/2}$	9.2×10^8	3.9×10^9	95
K	23.81	23.818[d]	$(2p^63d)^2D_{3/2}$–$2p^5(3s4s^3S)^2P^\circ_{1/2}$ $(2p^63d)^2D_{5/2}$–$2p^5(3s4s^3S)^2P^\circ_{3/2}$	5.9×10^9 1.4×10^{11}	1.6×10^7 2.7×10^7	7
O	20.35	20.353[c]	$(2p^63s)^2S_{1/2}$–$2p^5(3s4s^3S)^2P^\circ_{1/2}$ $(2p^63s)^2S_{1/2}$–$2p^5(3s4s^3S)^2P^\circ_{3/2}$	5.9×10^9 1.4×10^{11}	6.6×10^8 9.1×10^8	43

[a] Hartree–Fock calculation using the RCN/RCG atomic-physics code.[12]
[b] Previously observed using projectile electron spectroscopy.[13]
[c] Previously observed using absorption spectroscopy.[14,15]
[d] Calculated using our experimental value for the upper level combined with values from National Bureau of Standards tables for the lower level.[16]

Table 4. Other Mg Lines Observed

Line	λ Experiment (nm)	λ Other Experiment (nm)	Identification	Intensity (arb. units)
		Mg III		
L	23.42	23.426[a]	$(2p^6)^1S_0$–$[(2p^5)^2P_{3/2}]3s^3P^\circ_1$	1250
M	23.18	23.173[a]	$(2p^6)^1S_0$–$[(2p^5)^2P_{1/2}]3s^1P^\circ_1$	2150
Q	18.84	18.853[a]	$(2p^6)^1S_0$–$[(2p^5)^2P_{3/2}]3d^3P^\circ_1$	1.5
R	18.70	18.720, 18.651[a]	$(2p^6)^1S_0$–$(2p^53d)^3D_1$ and $^1P_1$	14.5
S	18.32	18.297[a]	$(2p^6)^1S_0$–$[(2p^5)^2P_{3/2}]4s^3P^\circ_1$	28
T	18.24	18.223[a]	$(2p^6)^1S_0$–$[(2p^5)^2P_{1/2}]4s^3P$	42
V	17.18	171.89, 171.29, 170.81[a]	$(2p^6)^1S_0$–$2p^54d$	7.0
		Mg IV		
U	18.09	18.079, 18.061[b]	$(2p^5)^2P$ – $(2p^43s)^2P_{1/2,3/2}$	11
V	17.18	17.165, 17.231[b]	$(2p^5)^2P$–$(2p^43s)^2D_{5/2,3/2}$	7
		Other Lines		
A	30.38	30.378[c]	He II $(1s)^2S$–$(2p)^2P^\circ$	4
D	25.63	25.632[c]	He II $(1s)^2S$–$(3p)^2P^\circ$	1.5
J	24.31	–	Impurity	3
N	22.11	–	Mg	2
P	19.27	–	Mg	14

[a] Previous emission spectrum of Mg III.[17]
[b] Previous emission spectrum of Mg IV.[18]
[c] National Bureau of Standards tables.[16]

The line at 24.83 nm was identified as $2p^53s^2\ ^2P_{3/2} \rightarrow 2p^63s\ ^2S_{1/2}$ based on the accurate absorption measurements of Esteva and Mehlman.[14] Its other fine-structure component, the decay from $2p^53s^2\ ^2P_{1/2}^\circ$, was not completely resolved from the line at 24.66 nm. Because of this uncertainty, no wavelength was assigned to line H, Table 3. Decay from $2p^53s^2\ ^2P$ was observed in emission by Vukstich *et al.*[22] at 24.9 nm, but fine structure was not resolved. Although the branching ratio for emission in the XUV for this level is expected to be poor because of strong autoionization, emission is observed because of the favorable mechanism for excitation of this configuration through inner-shell ionization of ground-level Mg atoms. Autoionizing times and radiative-decay rates have also been calculated for this con-

Table 5. Na Laser

Storage level	$2p^5[(3s3p)^3P]^4S_{3/2}$	$\tau_{AI} = 2.4 \times 10^{-6}$ sec	$\tau_{rad} = 1.0 \times 10^{-7}$ s
Upper laser level	$[(2p^53s)^1P3d]^2D_{5/2}$	$\tau_{AI} = 4.5 \times 10^{-11}$ sec	–
Intercombination transfer	$2p^5[(3s3p)^3P]^4S_{3/2} \rightarrow [(2p^53s)^1P3d]^2D_{5/2}$	$\lambda = 312 \pm 0.7$ nm	gf = 0.011
Laser transition	$[(2p^53s)^1P3d]^2D_{5/2} \rightarrow (2p^63d)^2P$	$\lambda = 37.5$ nm	gf = 0.485
Laser-gain cross section at 1.2-cm^{-1} linewidth	$\sigma = 5.6 \times 10^{-14}$ cm^2	–	–

Table 6. Mg II Laser

Storage level	$(2p^53s3p)^4S_{3/2}$	$\tau_{AI} = 1.1 \times 10^{-5}$ sec	$\tau_{rad} = 4.8 \times 10^{-8}$ sec
Upper laser level	$2p^5(3s4s^3S)^2P^o_{1/2}$	$\tau_{AI} = 1.7 \times 10^{-10}$ sec	–
Intercombination transfer	$(2p^53s3p)^4S_{3/2} \rightarrow 2p^5(3s4s^3S)^2P^o_{1/2}$	$\lambda = 160 \pm 1$ nm	gf = 0.0171
Laser transition	$2p^5(3s4s^3S)^2P^o_{1/2} \rightarrow (2p^64s)^2S_{1/2}$	$\lambda = 23.72$ nm	gf = 0.0537
Laser-gain cross section at 1.5-cm^{-1} linewidth	$\sigma = 1.49 \times 10^{-14}$ cm^2	–	–

figuration by Petrini.[23] His results agree with ours to within a factor of 2.

The lines at 20.35 and 23.81 nm are attributed to decays from $2p^5(3s4s^3S)^2P_{1/2}$ to $2p^63s^2S_{1/2}$ and $2p^63d^2D_{3/2}$, respectively. In addition, we would expect to observe a decay to $2p^64s$ at 23.72 nm. This was not observed, perhaps because of the strong interfering emission from Mg III at 23.42 nm. The line at 20.35 nm was previously seen by Esteva and Mehlman[14] in absorption, and was initially attributed to the $2p^63s3d$ configuration. Subsequent calculations[15] identify it as belonging to the $2p^53s4s$ configuration.

The remaining lines in the spectrum are given in Table 4. These lines are principally from Mg III, Mg IV, and He II, which were present in our Ar buffer gas in trace amounts. The line at 17.18 nm is most likely an overlap of Mg III and Mg IV lines. The line at 24.31 nm was observed with the cell run cold in both Ar and He. The lines at 22.11 nm and 19.27 nm were present only when the cell was hot and are presumably due to Mg. The line at 19.27 nm could be due to the Mg II $(2p^53s^3P_1)5s[1, 1/2]$ line seen in absorption at 19.284 nm.[14]

5. IMPLICATIONS FOR LASERS

The relatively intense emission of the $2p^53s3p\ ^4S_{3/2}$ level of both Na I and Mg II indicates the presence of relatively large excited-level populations. Although their small A coefficients probably preclude direct lasing, these levels are well suited as storage levels for store and transfer systems. Tables 5 and 6 give the RCN/RGN code parameters for XUV store and transfer lasers in these systems. In both systems, the target levels as well as the storage levels have been identified in this study.

ACKNOWLEDGMENTS

The authors gratefully acknowledge helpful discussions with E. McGuire, A. Weiss, and R. Cowan and the assistance of D. Holmgren and D. Walker. The research described here was supported by the U.S. Army Research Office and the U.S. Air Force Office of Scientific Research.

* Present address, Department of Physics, University of California, Berkeley, California 94720.

REFERENCES

1. E. J. McGuire, "The L-MM Auger spectra of Na and Mg," Phys. Rev. A **14**, 1402–1410 (1976).
2. E. J. McGuire and M. A. Duguay, "Soft x-ray gain in the alkali earths," Appl. Opt. **16**, 83–88 (1977).
3. S. E. Harris, "Proposal for a 207-Å laser in lithium," Opt. Lett. **5**, 1–3 (1980).
4. R. W. Falcone and K. D. Pedrotti, "Pulsed hollow-cathode discharge for extreme-ultraviolet lasers and radiation sources," Opt. Lett. **7**, 74–76 (1982); R. W. Falcone, D. E. Holmgren, and K. D. Pedrotti, "Hollow-cathode discharge for XUV lasers and radiation sources," AIP Conf. Proc. **90**, 287–295 (1982).
5. D. E. Holmgren, R. W. Falcone, D. J. Walker, and S. E. Harris, "Measurement of lithium and sodium metastable quartet atoms in a hollow-cathode discharge," Opt. Lett. **9**, 85–87 (1984).
6. D. E. Holmgren, D. J. Walker, D. A. King, and S. E. Harris, "Laser spectroscopy of Na I quartets," Phys. Rev. A **31**, 677–683 (1985).
7. J. A. R. Samson and R. B. Cairns, "Photoelectric yields of metals in the vacuum ultraviolet," GCA Tech. Rep. No. 66-17-N (NASA-CR-94614) (1966).
8. P. Jelinsky, C. Martin, R. Kimble, S. Bowyer, and G. Steele, "Composite thin-foil bandpass filter for EUV astronomy: titanium–antimony–titanium," Appl. Opt. **22**, 1227–1231 (1983).
9. A. W. Weiss, National Bureau of Standards, Washington, D.C. 20234 (personal communication).
10. J. Sugar, T. B. Lucatorto, T. J. McIlrath, and A. W. Weiss, "Even-parity autoionizing states in neutral sodium (350–400 Å)," Opt. Lett. **4**, 109–111 (1979).
11. R. L. Kelly and L. J. Palumbo, "Atomic and ionic emission lines below 200 Å," Rep. No. 7599 (U.S. Naval Research Laboratory, Washington, D.C., 1973).
12. R. D. Cowan, *The Theory of Atomic Structure and Spectra* (U. California Press, Berkeley, Calif., 1981), Secs. 8-1, 16-1, and 18-7.
13. D. J. Pegg, H. H. Haselton, R. S. Thoe, P. M. Griffin, M. D. Brown, and I. A. Sellin, "Core-excited autoionizing states in the alkali metals," Phys. Rev. A **12**, 1330–1339 (1975).
14. J. M. Esteva and G. Mehlman, "Autoionization spectra of magnesium (Mg I, Mg II, and Mg III) in the 50- to 110-eV energy range," Astrophys. J. **193**, 747–753 (1974).
15. G. Mehlman, A. W. Weiss, and J. M. Esteva, "Revised classification of Mg II levels between 59 and 63 eV," Astrophys. J. **209**, 640–641 (1976).
16. C. E. Moore, *Atomic Energy Levels* (U.S. Government Printing Office, Washington, D.C., 1949), Vol. I.
17. T. Lundström, "Ground term combinations of Mg III," Phys. Scr. **7**, 62–64 (1973).
18. G. A. Johannesson, T. Lundström, and L. Minnhagen, "Extended analysis of the spectrum of Mg IV," Phys. Scr. **6**, 129–137 (1972).
19. J. R. Willison, "Spontaneous and laser-induced XUV radiation

from core-excited lithium atoms and ions," Ph. D. dissertation, G. L. Rep. No. 3434 (Edward L. Ginzton Laboratory, Stanford University, Stanford, Calif., 1982).
20. Yu. V. Zhmenyak, V. S. Vukstich, and I. P. Zapesochnyi, "Radiative decay of Na I autoionization states excited in electron–atom collisions," JETP Lett. **35,** 393–396 (1982).
21. S. E. Harris, D. J. Walker, R. G. Caro, A. J. Mendelsohn, and R. D. Cowan, "Quasi-metastable quartet levels in alkalilike atoms and ions," Opt. Lett. **9,** 168–170 (1984).
22. V. S. Vukstich, Yu. V. Zhmenyak, and E. N. Postoi, "Radiative decay of certain autoionized states of Mg I and Mg II," JETP Lett. **30,** 261–265 (1979).
23. D. Petrini, "Theoretical Auger rates for the $'2p^5 3s^{2'}$ levels: sodium and magnesium atoms," J. Phys. B **14,** L617–L621 (1981).